

## Clinical pathology of kidney disease

- Kidney disease is typically diagnosed using light microscopy, immunohistology and electron microscopy (EM).
- EM is useful in the histopathology of ~50% of native kidney biopsies and essential for the diagnosis of ~20% and is a standard technique for diagnosis of kidney disease in many countries. EM is particularly useful for the diagnosis of kidney diseases associated with structural abnormalities of the basement membrane (e.g. inherited abnormalities of collagen type IV alpha chains), diseases with fibrils (e.g. fibrillary and immunotactoid glomerulonephritides) and rare genetic diseases such as Fabry's disease or lecithin cholesterol acyl transferase (LCAT) deficiency.
- EM is also routinely used to document morphological changes in podocytes, and the shape, substructure and position relative to the glomerular basement membrane (GBM) of immune complexes and/or complement fragment deposits.
- The relatively high costs associated with the equipment and the need for specialist staff mean that diagnostic EM is not accessible for most of the world's population.
- Recent progress in single molecule localisation microscopy now enables conventional widefield fluorescence microscopes to be adapted at modest cost to provide super-resolved immunofluorescence with resolution below 50 nm in biological specimens.
- We have applied stochastically switched optical reconstruction microscopy (STORM) to clinical histological sections stained with standard immunofluorescence techniques to explore whether super-resolved immunofluorescence imaging ("histoSTORM") can provide a means to resolve ultrastructure to aid the diagnosis of kidney disease where EM is not available. This initial work has been published<sup>1</sup> in J Pathology: Clinical Research at <http://doi.org/10.1002/cjp2.217>.

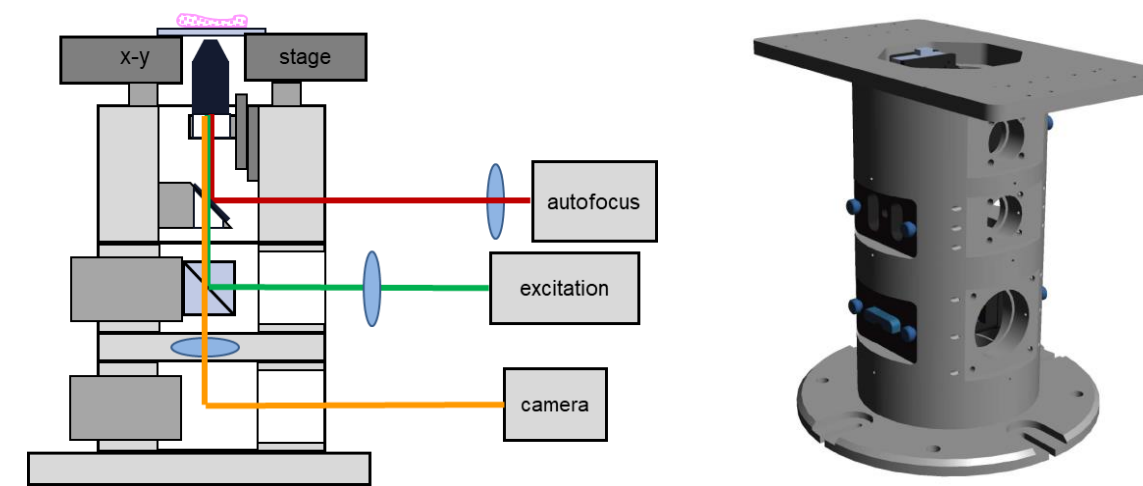
## Low-cost super-resolved fluorescence microscopy

### STORM Microscopy

- Structural features smaller than 0.2  $\mu\text{m}$  are not resolved with conventional fluorescent microscopy
- In stochastic optical reconstruction microscopy (STORM) individual fluorescent molecules are localised with high accuracy.
- Frozen or paraffin embedded kidney tissue is stained with conventional immunofluorescence and, upon exposure to sufficiently high intensity irradiation, the fluorophores can be stochastically switched between a non-fluorescent and fluorescent state.
- The same region of interest is imaged every 30 milliseconds over 5000 frames (STORM movie). At every frame, most of fluorescent labels are switched off and the fluorophores in the on state are well separated and distinguishable.
- An intensity peak-finding algorithm identifies the peaks/molecules in each frame and a list of fluorophore positions is stored as a table of localised molecules.
- Dynamic rendering allows reconstruction of the STORM image using the points features stored in the table of localised molecules.
- A platform for STORM microscopy easySTORM<sup>2</sup> has been developed and adapted for diagnosis of human glomerular diseases in clinical settings.

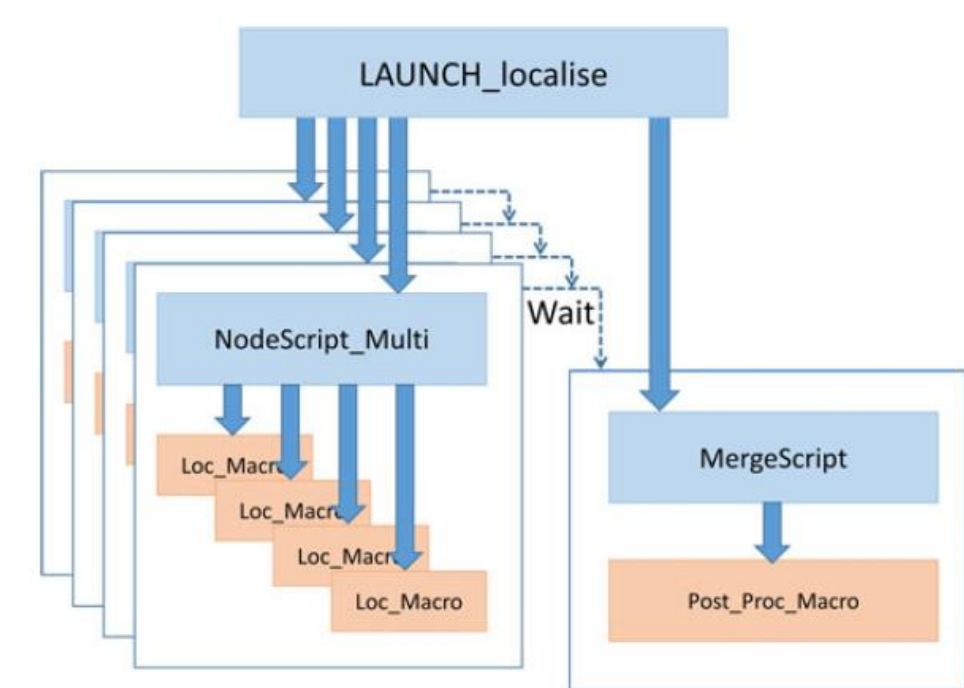
### Low-cost implementation possible on openFrame platform

- integrating piezo z-drive module,
  - self-built optical autofocus<sup>5</sup>
  - multiline excitation laser bank (~£500 per laser line),
  - CMOS camera,
  - low-cost optical components
- [www.openScopes.com](http://www.openScopes.com)



### Parallelised STORM data processing on HPC<sup>6</sup>

- Single-molecule localisation of data from one field of view can be processed e.g. using ThunderSTORM, and can be parallelised across multiple HPC nodes (and multiple instances on each node)
- or
- Single molecule localisation of data from multiple fields of view can be processed in parallel, e.g. using ThunderSTORM, on multiple HPC nodes (and on multiple instances on each node)



## histoSTORM: super-resolved immunofluorescence of histological sections

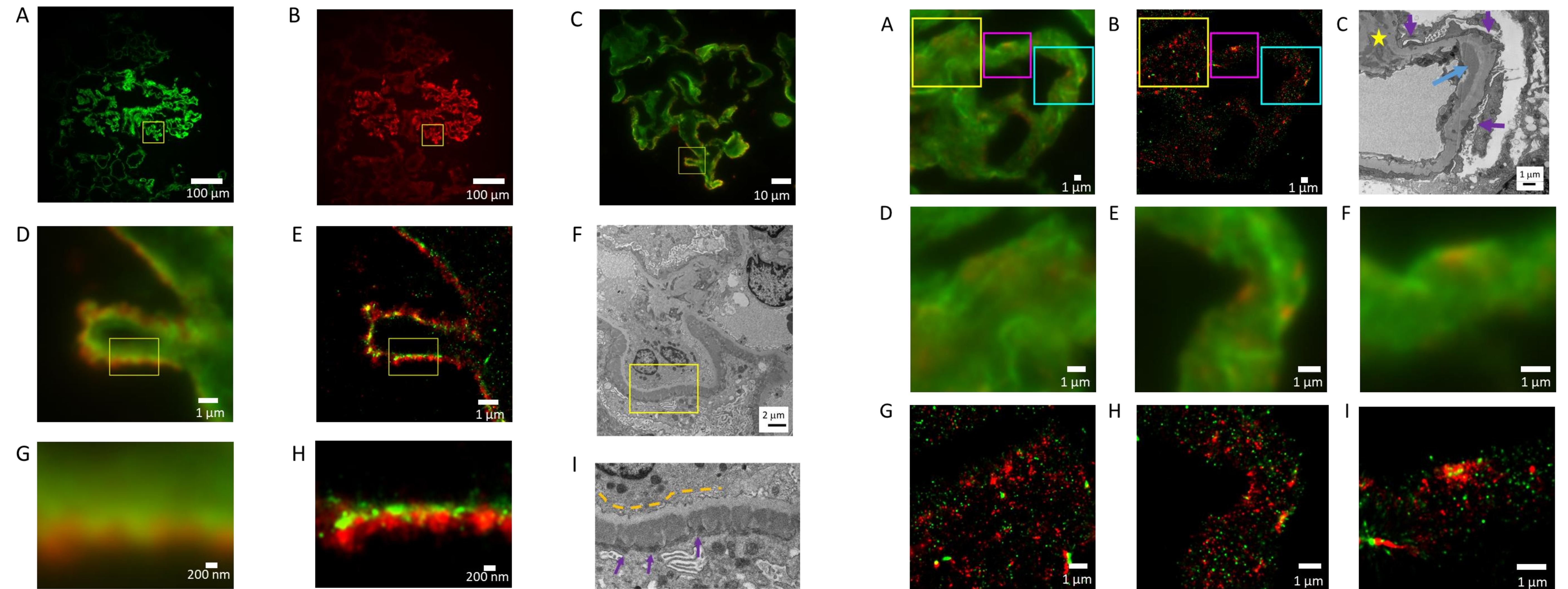


Figure 1. Frozen section presenting Membranous Glomerulonephritis

Basement membrane (laminin, green – Alexa Fluor 555), immunoglobulin G deposits (IgG, red – iFluor 647). **A-B** Widefield immunofluorescence images at 4x magnification of frozen section of Membranous Glomerulonephritis showing **A**: laminin channel, **B**: IgG channel, and **C**: 100X two-channel image of region indicated by yellow square in **A** and **B**. **D**: Widefield immunofluorescence of region indicated by yellow square in **C**; **E**: Corresponding STORM image with pixel size rendered at 25 nm. **F**: Electron micrograph of similar structure from same biopsy at 20,200x magnification. **G**: Widefield immunofluorescence image of 3.2 x 2.4  $\mu\text{m}^2$  region indicated in **D,E** with **H**: corresponding STORM image; **I**: expanded electron micrograph image of region indicated in **F**. Yellow dashed lines indicate the light grey glomerular basement membrane. Dark grey electron-dense deposits on the sub-epithelial side (purple arrows) represent immune complexes containing IgG. (Figure adapted from Reference 1)

Figure 2. presenting Lupus Nephritis Type IV

Basement membrane (laminin, green – Alexa Fluor 555), immunoglobulin G deposits (IgG, red – iFluor 647) **A**: Widefield immunofluorescence image at 100x magnification of frozen section presenting Lupus Nephritis Type IV with selected regions presenting **D,G**: Mesangial deposits, **E,H**: subendothelial deposits and **F,I**: subepithelial deposits. **B**: STORM image rendered with pixel size of 25 nm corresponding to **A**. **C**: Electron micrograph of similar structure from same sample, 30,400x magnification, presenting occasional electron dense deposits containing IgG on the subepithelial side of the glomerular basement membrane (purple arrows), on the subendothelial side of the glomerular basement membrane (blue arrow) and in the mesangium (yellow star). **G,H,I**: STORM images corresponding to wide-field immunofluorescence images of **D,E,F**. **D,G** show the region indicated by the yellow square in **A,B**. **E,H** show the region indicated by the cyan square in **A,B**. **F,I** show the region indicated by the purple square in **A,B**. (Figure adapted from Reference 1)

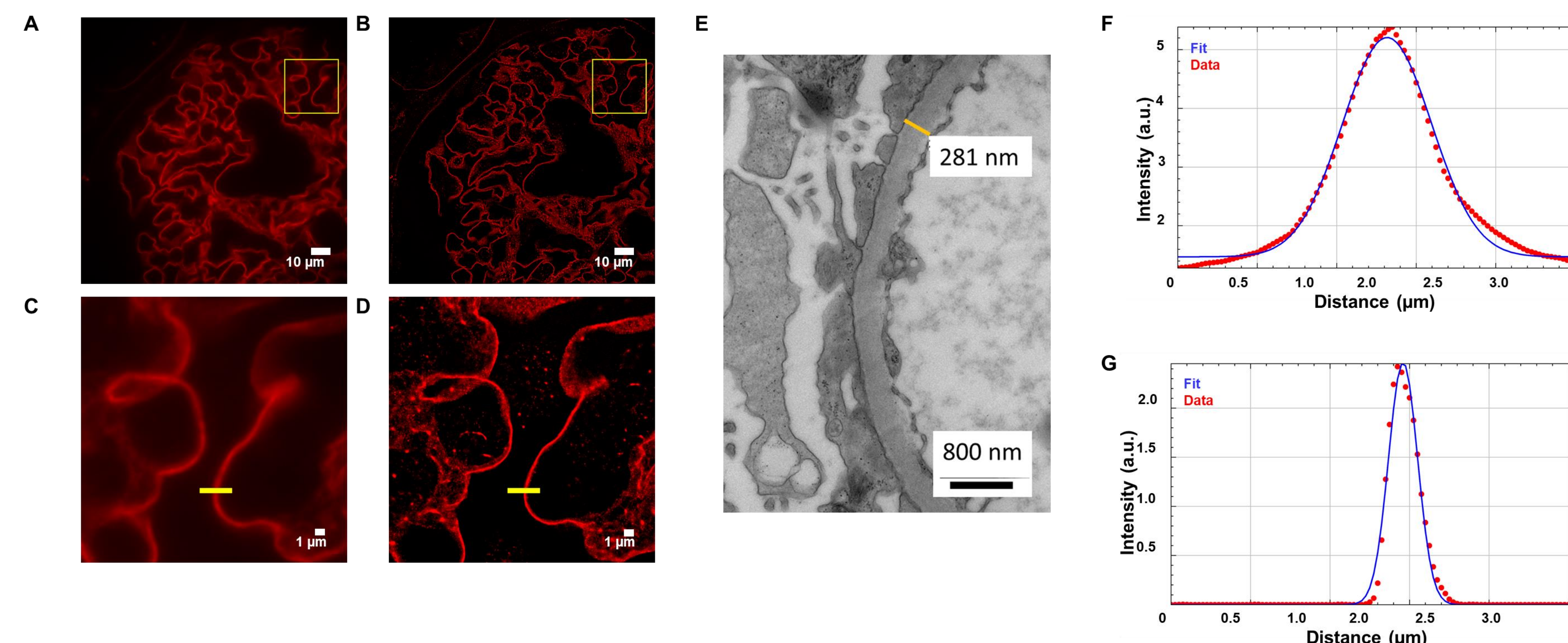


Figure 3. FFPE section presenting Minimal Change Disease

Glomerular basement membrane (Laminin-iFluor 647) **A**. Widefield immunofluorescence image at 100x magnification of FFPE section. **B**: Rendered STORM image of region shown in **A**. **C**: Widefield inset of a region shown in **A**. **D**: STORM inset of region shown in **B** rendered with a pixel size of 25 nm **E**. Electron micrograph of a GBM from different section of same biopsy, 60,700x magnification, for which the GBM thickness at indicated position is 281 nm. **F**: Presenting measured thickness (full width at half maximum) of GBM from wide-field immunofluorescence image **C** line profile (657 nm) **G**: Measured thickness (full width at half maximum) of STORM image **D** at line profile (212 nm). (Figure adapted from Reference 1)

## Summary

- *histoSTORM* of frozen or FFPE kidney biopsy sections can provide additional information compared to conventional widefield immunofluorescence, e.g. locating subepithelial, subendothelial and mesangial immune complex deposits, which can aid the diagnosis of glomerulonephritis,
- *histoSTORM* enables the thickness of the GBM to be measured with sufficient resolution to aid diagnostic assessments where EM is not available
- The sample preparation for *histoSTORM* is similar to immunofluorescence
- *histoSTORM* is cheaper and easier to implement and sustain than EM, and so has the potential to improve the diagnosis of kidney disease in a much wider range of clinical settings.

## Acknowledgements

The authors thank Dr Linda Moran from North West London Pathology for her expertise in electron microscopy. We gratefully acknowledge funding from the Imperial College Confidence in Concept fund supported by the Medical Research Council and the Wellcome Trust, from a Research England GCRF Institutional Award and the Imperial College London Impact Acceleration Accounts supported by the Biotechnology and Biological Sciences Research Council (EPSRC EP/R51547/1). CAR's research activity is made possible with generous support from Sacharh and Indra Burman and is supported by the National Institute for Health Research (NIHR) Biomedical Research Centre based at Imperial College Healthcare NHS Trust and Imperial College London. Infrastructure support for this research was provided by the NIHR Imperial Biomedical Research Centre. SK and YA are supported by funding from the Francis Crick Institute, which receives its core funding from Cancer Research UK (FC001003), the UK Medical Research Council (FC001003) and the Wellcome Trust (FC001003). JL acknowledges a PhD studentship from EPSRC. Tissue samples were provided by the Imperial College Healthcare NHS Trust Tissue Bank funded by the NIHR Biomedical Research Centre based at Imperial College Healthcare NHS Trust and Imperial College London.

## References

1. Garcia et al. J Pathology: Clinical Research (2021)
2. Kwakwa et al. J Biophotonics 9 (2016) 948
3. Heilmann et al. Angewandte Chemie Int Ed 47 (2008) 6172
4. Fölling et al. Nature Methods 5 (2008) 843
5. Lightley et al. J Microscopy, in press: <https://doi.org/10.1111/jmi.13020>
6. Munro et al. J Microscopy 273 (2018)148